5. Diffraction of X-Rays by Imperfect Crystals and Paracrystals

5.1 Ideal Crystals and Imperfect Crystals

The term "crystalline" as we have so far used it in this volume has usually referred to ideal crystals with perfectly regular arrangements of atoms. High polymer solids are often referred to as crystalline, but, unlike ionic crystals or metals, the internal atomic arrangement is by no means as simple as this might imply. Although direct observation of the internal arrangement is impossible, reliable inferences from physical and chemical evidence lead us to believe that high polymers consist of various regions, each with a characteristic degree of internal order, ranging continuously from something close to the ideal crystalline state to the completely amorphous state.[†1] Chain polymers, for example, can exhibit a very wide variety of arrangements, with varying degrees of disorder. Even in one and the same highly crystalline region of such a substance the arrangement of the atoms and molecules is not always perfectly regular, and even in amorphous regions there are often areas in which the molecules are roughly parallel to one another, *i.e.* in which the arrangement is quasi-crystalline.[†2] This complexity of polymer structure means that the distinction between a substance which forms "ideal" crystals and that which is merely "crystalline" must be clearly drawn when referring to polymers. Cotton, silk, and nylon are "crystalline" high polymers. However, the crystalline regions of these substances are not "crystals" in the strict sense, and are more generally referred to as "paracrystals". The X-ray diffraction patterns of these materials give further evidence of a variety of atomic arrangements, in that they contain elements which range from those more characteristic of a crystal with a perfect lattice to those resembling the diffuse halos given by amorphous substances. Three examples of such patterns are given in Fig. 5.1. The order of decreasing crystallinity is from left to right.

There is another state which is regarded as crystalline, but in which the crystals are soft and plastic like wax. Substances in this state are known as plastic crystals. While the positions of the molecules in the crystal remain unchanged, the molecules as a whole, or their side chains, rotate, weakening the intermolecular interactions to give these crystals plasticity and other characteristic properties. Liquid crystals, either nematic, smectic, or cholesteric, are formed mostly by rod-like molecules. At elevated temperatures before melting, a regular arrangement of molecules in a crystalline state is disturbed by thermal motions of their end, side chain groups, or others, changing the crystal into a liquid crystalline mesophase (thermophilic liquid crystal). In lyophilic liquid crystals, this kind of disorder is caused by water or solvent molecules penetrated into the crystalline lattice, instead of thermal agitations. Their unique structures and properties are known well. Discotic mesophase mostly formed by disc-shaped molecules is also one of the mesophases between crystal and liquid (or solution) phases.

[†1] We have to write here as "*non-crystalline* solid state" instead of amorphous state. Originally, "*amorphous*" means a-morphous (non morphological shape, non-crystalline.). "Amorphous" also means that the state in question belongs to a non-equilibrium state. However, the word "amorphous" is customarily and widely used in the field of high polymer science to mean non-crystalline. Accordingly, in this volume the word "amorphous" is used instead of "non-crystalline."

[†2] Not to be confused with the "quasicrystal," which was first discovered in rapidly solidified Al-Mn alloys.[1] The quasicrystals examined hitherto show icosahedral symmetry, or eight-, ten-, or twelve-fold symmetry. The discovery of quasicrystals has stimulated considerable research activity mainly because it appears to violate the classical rules of crystallography.

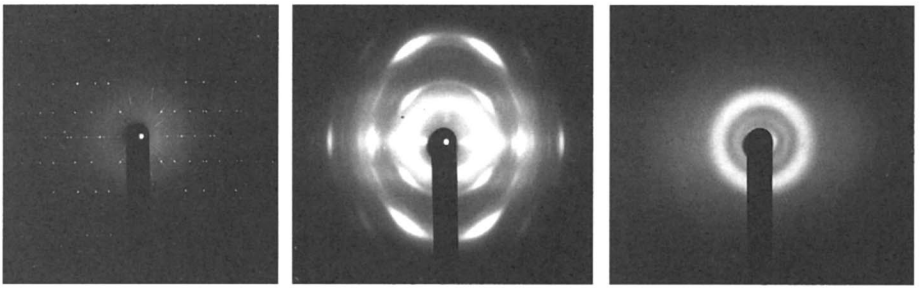

(a) (b) (c)

Fig. 5.1 Examples of X-ray diffraction diagrams of a single crystal and high polymer substances of varying crystallinity (cylindrical film).
(a) Dimethyltin bis(dithiocarbamate) (Oscillation photograph, single crystal); (b) Polyvinylidene-fluoride (Fiber diagram, draw direction vertical); (c) Curdlan (or β-(1→3)-D-glucan).

Figure 5.2 is an attempt to illustrate these states using representative points for the unit assemblages of atoms or molecules. In the case of a high polymer the representative point corresponds to the repeating unit, *e.g.* -CH_2-CH_2- for polyethylene. Diagram (a) in Fig. 5.2 shows the amorphous state, in which the arrangement is completely disordered; (d), at the opposite extreme, shows the ideal crystalline state, in which the atoms, ions or molecules have a completely regular arrangement in three dimensions. Crystals of substances having identical molecules of fixed shape can exhibit a very high degree of regularity; these are the so-called ideal crystals. To fall within this category, distortion of the arrangement within the crystal due to all operative factors should be such that the displacement of the lattice points from the ideal positions, expressed as a statistical average over the whole crystal, is

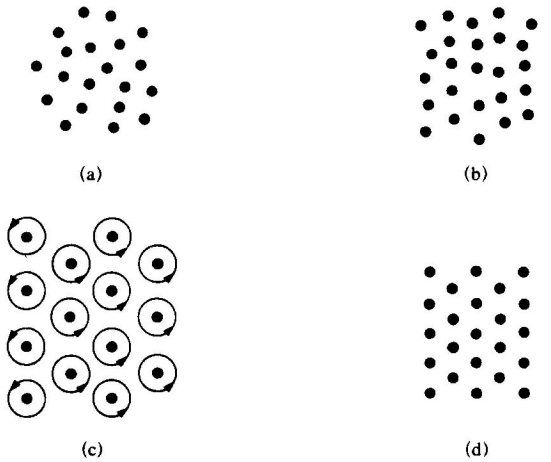

(a) (b) (c) (d)

Fig. 5.2 Schematic representation of atomic and molecular assemblages.
(a) Amorphous substance; (b) Paracrystal; (c) Plastic crystal (circular arrow indicates the rotation of each molecule around its center of gravity); (d) Crystal.

(say) less than 1% of the repeat distance (*cf.* Fig. 15.30). The crystalline state which is "perfect" within this 1% limit is more likely to be observed in substances of low molecular weight, where incipient distortion is generally corrected under the equilibration of the interparticle forces within the solid.

The situation is different, however, with high polymers. It is particularly improbable that the molecular arrangement in the fibrous solids formed by linear chain polymers should be that of an ideal crystal as shown in Fig. 5.2(d). The crystal structures of various high polymers beautifully drawn in many textbooks are all ideal structures, and may be far from the real structure. In long chain macromolecules and very large three-dimensional ions such as are found in glasses, all atoms may not have time to assume the arrangement with the highest degree of crystallinity before they are "frozen" into position by the rapid cooling of the melt. Again, there may be thermodynamic factors which make the state with residual distortion inherently stable. This kind of imperfection is represented by Fig. 5.2(b). Diagram (c) in Fig. 5.2 represents a plastic crystal.

A classification of crystal imperfections (lattice distortions) follows.

5.1.1 Lattice distortions of the first kind

A. Thermal vibration

The lattice points constitute an ideal crystal, but there is continuous thermal vibration about the lattice points. The ideal crystalline lattice is, however, maintained by the equilibrium positions of the atoms (Fig. 5.3(b)).

B. Frozen structure

The lattice points are displaced away from their theoretical positions, the displacements being small compared with the interatomic distances, but the average lattice in the crystal is

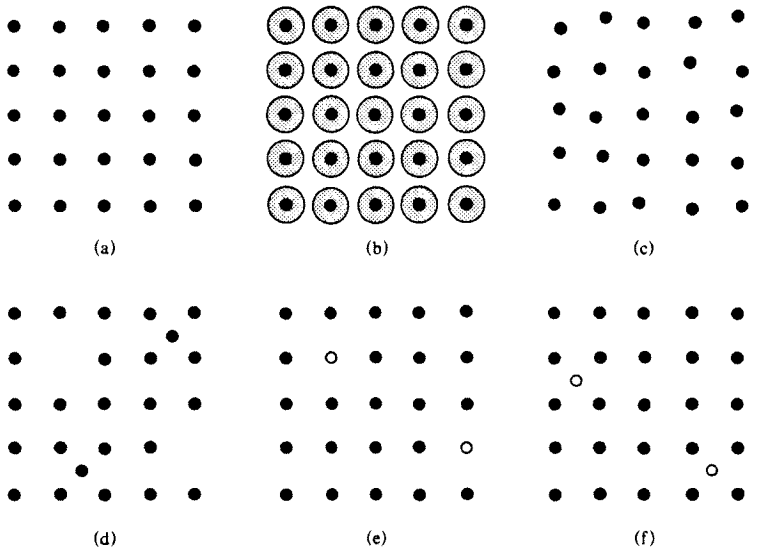

Fig. 5.3 Schematic representation of distortions of the first kind.
(a) Ideal two-dimensional crystal lattice, (b) Thermal motion, (c) Frozen thermal motion, (d) Defect lattice (vacancies and interstitials), (e) Mixed crystal or solid solution (substitution type), (f) Mixed crystal or solid solution (interstitial type).

ideally maintained. This imperfection corresponds to a thermally vibrating crystal lattice, the structure of which has been frozen at a certain instant (Fig. 5.3(c)).

C. Vacancies and interstitials

Most of the lattice points are correctly positioned, but a small number of atoms are missing from the lattice points, or a small number of extra atoms are inserted into the lattice but not on regular lattice sites (Fig. 5.3(d)).

D. Mixed crystals or solid solutions

The atoms, atomic groups, ions, or molecules forming the crystal are not all of the same type, but are a substituted mixture of different components which, on average, form an ideal lattice (Fig. 5.3(e) and (f)).

E. Dislocations

Edge and screw dislocations (Fig. 5.4)[2] are typical one-dimensional defect of the atomic (or molecular) arrangement in crystals. In the top half of the Fig. 5.4 a_1), a projection of a distorted structure looks like as if an extra atomic net plane is inserted perpendicular to the paper like a knife edge (edge dislocation). By shear the slip runs to left (or right) along with the broken line between the upper and lower structures, and the dislocation moves (*cf.* Fig. 5.5(f)). Fig. 5.4 b_1) and b_2) show that the mistake of the atomic arrangement is helical

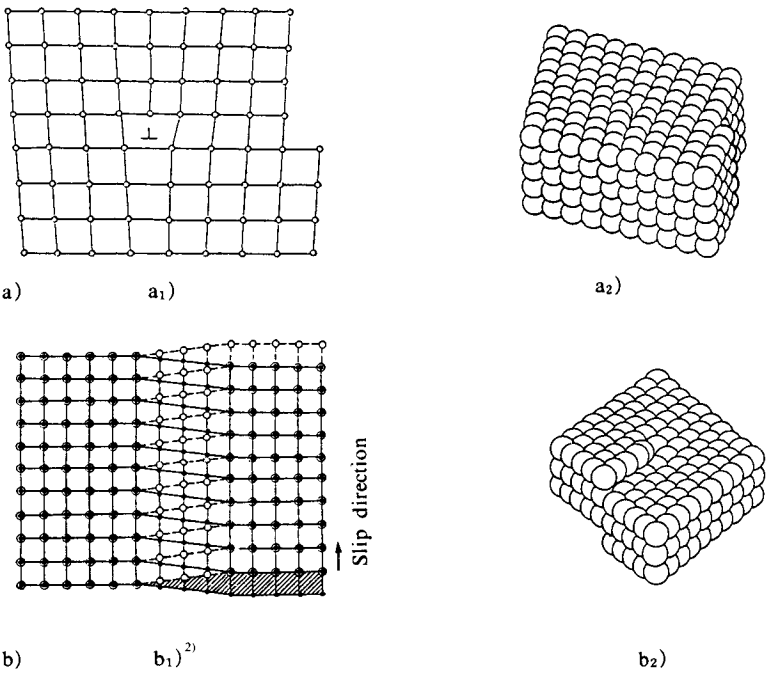

Fig. 5.4 Dislocations.
(a) Edge dislocation: a_1) Section showing a mistake of atomic arrangement along with an edge dislocation; ($\perp$ denotes that one atomic net plane is excess above this mark), a_2) Three-dimensional model
(b) Screw dislocation: b_1) Section showing an imperfection of atomic arrangement along with a screw dislocation (small white and black circles represent atoms above and below the slip plane, respectively); b_2) Three-dimensional model.
b_1): [Reproduced from W. T. Read, Jr, *Dislocations in Crystals*, p. 17, McGraw-Hill (1953)]
a_2), b_2): [Reproduced with permission from S. Koda, *Introduction to Metal Physics* (Revised ed.), pp. 134, 135, Corona Pub. (1973)]

along the central, vertical line (screw dislocation). In this dislocation, the slip direction of atoms is parallel to dislocation line (*cf.* Fig. 7.11(b_2)).

Basic defects in crystalline regions of high polymer substances are also schematically shown in Fig. 5.5. In a regular arrangement of high polymer chain molecules, there is a defect where the number of repeating units of a chain is more (or less) than the other near-by polymer chains (Fig. 5.5(a)). Fig. 5.5(b) shows an interchange, but not a crossing, of two adjacent chains. A defect caused by a pair of back-foldings of chain molecules is illustrated in Fig. 5.5(c). Back-folding(s) or end(s) of polymer chains also make a defect (Fig. 5.5(d) and (e)). Fig. 5.5(f) may be considered formed from (d) or (e) by the successive movement of adjacent polymer chains to fill vacancies, which may be considered as a movement of an edge dislocation.

The above imperfections of crystals introduce fluctuations into the distances between corresponding atoms throughout the substance, but preserve a long-range order which is distributed only to about the same extent as the short-range order.

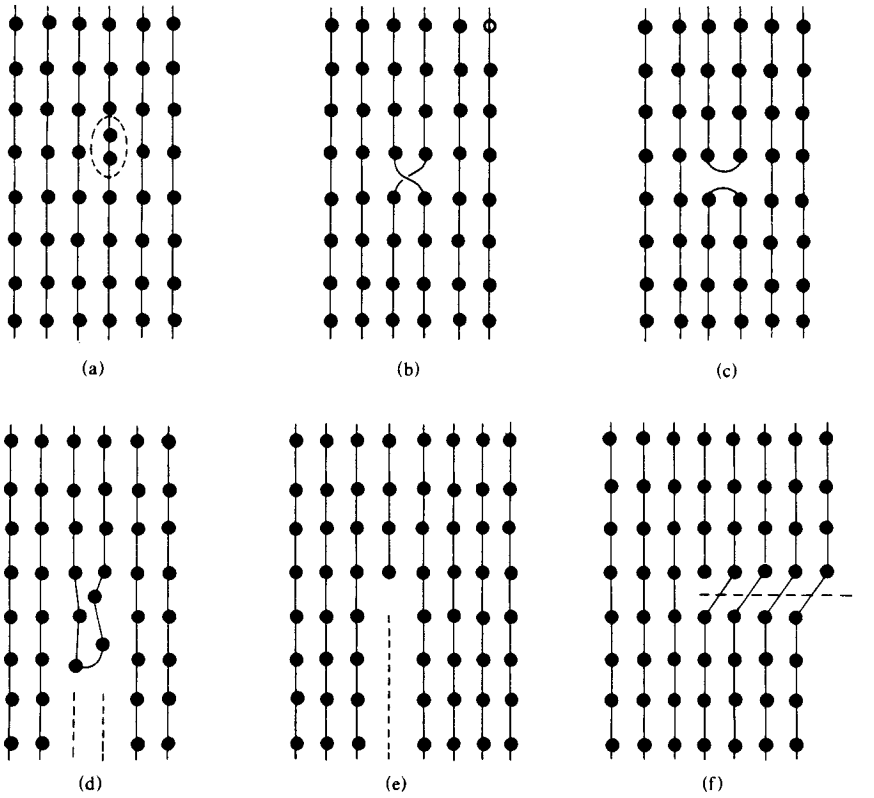

Fig. 5.5 Schematic illustration of basic defects in high polymer crystalline regions (*cf.* Fig. 7.18). (Small black circles represent repeating units in high polymer chain molecules).
(a) Mistake of the number of repeating units, (b) Spatial interchange of adjacent polymer chains, (c) Backfoldings of polymer chains, (d) Backfolding of polymer chain and vacancy, (e) End of polymer chain and vacancy, (f) Kinking of polymer chain to fill vacancy followed by moves of vacancy.

5.1.2 Lattice distortions of the second kind

Whereas the average positions of all the representative points in distortions of the first kind correspond to the lattice points of an ideal crystal, there is a further kind of distortion in which not even the statistical averages of the positions of the representative points form an ideal lattice, the distortion being so great that they deviate significantly from the ideal lattice positions. Three-dimensional periodicity resembling that of an ideal crystal only persists over short ranges; over long ranges there is a permanent disorder resembling that of the amorphous state. These are known as distortions of the second kind, and it is this type of imperfection which Hosemann introduced as paracrystalline.[3,4] In one sense this classification applies to all types of structure intermediates between the ideal crystal and amorphous states. It also, however, covers those mixtures of crystalline and amorphous regions with continuous mutual gradation which are formed by chain molecules, so that the entire non-homogeneous structure may properly be described as paracrystalline.

These different types of distortion are illustrated in Fig. 5.6,[5] in which, again, only the representative points are shown. Fig. 5.6 a_1) shows an ideal oblique crystal lattice. The lat-

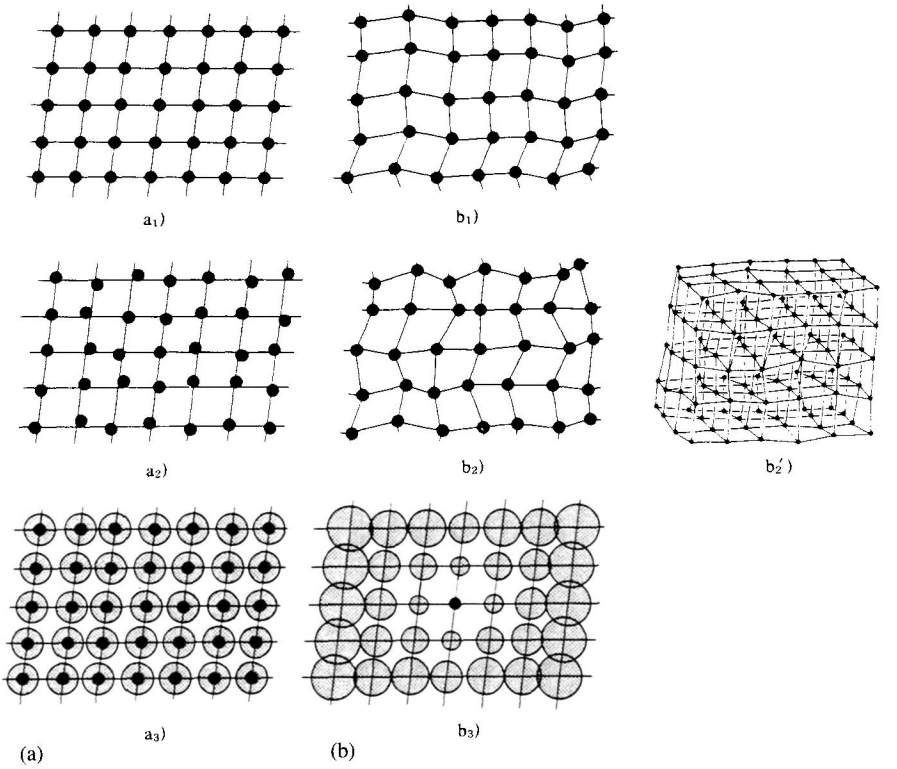

Fig. 5.6 Schematic representation of distortions of the second kind compared with distortions of the first kind. (a) Distortion of the first kind: a_1) Ideal oblique two-dimensional lattice,[5] a_2) Distortion of the first kind (frozen thermal motion),[5] a_3) Distribution function of the first kind.[5] (b) Distortion of the second kind; b_1) Ideal paracrystalline lattice,[5] b_2) General paracrystalline lattice,[5] b_2') General paracrystalline lattice (three-dimensional), b_3) Distribution function of the second kind[5] a_2), b_2), a_3), b_3) : [Reproduced with permission from B. K. Vainshtein, *Diffractions of X-rays by Chain Molecules*, p.97, Elsevier (1966)]

tice in b_1) still appears to possess the regularity of a crystal lattice. All unit cells are parallelpipeds (parallelograms in this two-dimensional representation), so the vectors in any sequence, *e.g.* left to right, bottom to top, are always parallel and equal in continuous part (an ideal paracrystalline lattice: lattice distortion of the second kind). Fig. 5.6 a_2) again illustrates the frozen structure of thermal vibration in an ideal crystal; the positions of the atoms fixed at an instant are denoted by the small black circles. In b_2) the lattice is still discernible with the aid of the lines joining the points, but if the lines were removed, the arrangement would be practically indistinguishable from the amorphous state (a general paracrystalline lattice). Fig. 5.6 b_2') depicts a three-dimensional, general paracrystalline lattice. In the paracrystalline lattice we assume that we can clearly trace the three main directions or three axes corresponding to those of the crystal, that each of these directions is a continuation of paracrystalline unit cell vector $\boldsymbol{a}$, $\boldsymbol{b}$, or $\boldsymbol{c}$, the values and directions of which differ slightly from cell to cell, and that these directions do not fold back and never cross spatially. Fig. 5.6 a_3) and b_3) respectively show distribution function for the lattice distortions of the first and the second kinds.

This concludes our brief description of the paracrystalline state, but since the analytical methods we have so far developed are inadequate to explain X-ray diffraction by such substances, it is necessary to introduce Fourier transform theory.

5.2 Fourier Transform Theory of X-Ray Diffraction

5.2.1 Fourier transform theorem

Our discussion of X-ray diffraction theory has so far been confined mainly to simple methods for calculating the amplitudes of X-rays diffracted from substances with various atomic structures. These are the most general ways of treating X-ray diffraction phenomena, although there is another straightforward way (applicable only to diffractions from crystals) which finds a place in most works on the subject. A far more refined mathematical analysis is needed, however, to explain the diffraction of X-rays by more complex structures, such as the paracrystalline substances dealt with in this chapter. A simple exposition of the fundamentals of Fourier transform theory as it applies to X-ray diffraction follows. This should equip the reader to both interpret and apply X-ray diffraction from paracrystals and other substances.

The relationship between the structure of a substance (in terms of its electron density distribution) and the X-ray scattering amplitude was shown in Eqs. 2.13 and 2.14. Eq. 2.13 shows how the amplitude $A(\boldsymbol{S})$ of the scattered X-rays may be derived from the structure of the substance $\rho(\boldsymbol{r})$ by phase-dependent integration of the contributions from all elements of the system:

$$A(\boldsymbol{S}) = \int_0^\infty \rho(\boldsymbol{r}) \exp\{-2\pi i(\boldsymbol{S}\cdot\boldsymbol{r})\} \mathrm{d}v_r \tag{5.1}$$

According to the Fourier integral theorem, a function $F(\boldsymbol{S})$ in Fourier space is equal to the integral over real space of a function $\rho(\boldsymbol{r})$ in real space, *i.e.*

$$F(\boldsymbol{S}) = \int_0^\infty \rho(\boldsymbol{r}) \exp\{-2\pi i(\boldsymbol{S}\cdot\boldsymbol{r})\} \mathrm{d}v_r \tag{5.2}$$

Thus if $\rho(\boldsymbol{r})$ in Eq. 5.2 is a function representing the electron density of the atoms in a substance, it can be seen from the form of this equation that $F(\boldsymbol{S})$ corresponds exactly to the X-ray scattering amplitude $A(\boldsymbol{S})$ for the substance. From the inverse Fourier transform theo-

rem (Eq. 2.14), we may put

$$\rho(\boldsymbol{r}) = \int_0^\infty A(\boldsymbol{S})\exp\{2\pi i(\boldsymbol{S}\cdot\boldsymbol{r})\}\mathrm{d}v_s \tag{5.3}$$

The physical meaning of this is that the structure of a given substance is equivalent to the Fourier transform of its X-ray scattering amplitude. Using this theorem of Fourier transforms, we can take the mathematical analysis of X-ray diffraction a stage further.

As we saw earlier, the intensity of the scattered X-rays, in units of the scattering intensity of an electron, is simply

$$I(\boldsymbol{S}) = A(\boldsymbol{S})A^*(\boldsymbol{S}) = |A(\boldsymbol{S})|^2 \tag{5.4}$$

Let us now examine the Fourier transform of this intensity I.

$$\begin{aligned} Q(\boldsymbol{r}) &= \int_0^\infty I(\boldsymbol{S})\exp\{2\pi i(\boldsymbol{S}\cdot\boldsymbol{r})\}\mathrm{d}v_s \\ &= \int_0^\infty A(\boldsymbol{S})A^*(\boldsymbol{S})\exp\{2\pi i(\boldsymbol{S}\cdot\boldsymbol{r})\}\mathrm{d}v_s \end{aligned} \tag{5.5}$$

Eq. 5.5 is simply derived using Eqs. 5.1 and 5.3. Another useful theorem will now be introduced.

For given functions $\rho(\boldsymbol{r})$ and $\sigma(\boldsymbol{r})$, the function $\rho(\boldsymbol{r}) * \sigma(\boldsymbol{r})$ defined by

$$\int_0^\infty \rho(\boldsymbol{y})\sigma(\boldsymbol{r}-\boldsymbol{q})\mathrm{d}v_q = \rho(\boldsymbol{r}) * \sigma(\boldsymbol{r}) \left(=\widetilde{\rho(\boldsymbol{r})\sigma(\boldsymbol{r})}\right) \tag{5.6}$$

is known as the convolution of $\rho(\boldsymbol{r})$ and $\sigma(\boldsymbol{r})$, and the corresponding operation is known as convolution or folding, denoted by $*$ (or $\frown$) in the place of a multiplication sign. A two-dimensional illustration of this mathematical operation is given in Fig. 5.7.

If $A(\boldsymbol{S})$ and $S(\boldsymbol{S})$ are Fourier transforms of $\rho(\boldsymbol{r})$ and $\sigma(\boldsymbol{r})$ respectively, the Fourier transform of the product of $\rho(\boldsymbol{r})$ and $\sigma(\boldsymbol{r})$ is

$$\int_0^\infty \rho(\boldsymbol{r})\sigma(\boldsymbol{r})\exp\{-2\pi i(\boldsymbol{S}\cdot\boldsymbol{r})\}\mathrm{d}v_r = \int A(\boldsymbol{S}')S(\boldsymbol{S}-\boldsymbol{S}')\mathrm{d}v_{s'} = A(\boldsymbol{S}) * S(\boldsymbol{S}) \tag{5.7}$$

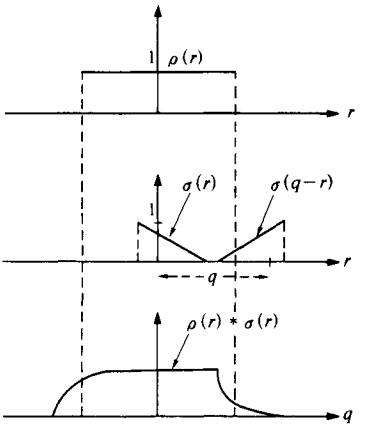

Fig. 5.7 The convolution operation on two functions $\rho(\boldsymbol{r})$ and $\sigma(\boldsymbol{r})$.

Thus the Fourier transform of the product of the functions is the convolution of their respective Fourier transforms $A(\boldsymbol{S})$ and $S(\boldsymbol{S})$. The inverse theorem is therefore

$$\int_0^\infty A(\boldsymbol{S}) * S(\boldsymbol{S}) \exp\{2\pi i(\boldsymbol{S}\cdot\boldsymbol{r})\}\mathrm{d}v_s = \rho(\boldsymbol{r})\cdot\sigma(\boldsymbol{r}) \tag{5.8}$$

i.e. the Fourier transform of a convolution is equal to the product of the Fourier transforms of the respective functions.

Let us now return to Eq. 5.5. Since $Q(\boldsymbol{r})$ is the Fourier transform of the product of two functions $A(\boldsymbol{S})$ and $A^*(\boldsymbol{S})$, application of the theorem of Eq. 5.7 to Eq. 5.5 gives

$$Q(\boldsymbol{r}) = \int \rho(\boldsymbol{q})\rho(\boldsymbol{r}+\boldsymbol{q})\mathrm{d}v_q = \rho(\boldsymbol{r}) * \rho(\bar{\boldsymbol{r}}) \tag{5.9}$$

$Q(\boldsymbol{r})$ is the self convolution of $\rho(\boldsymbol{r})$. In physical terms, when the vector $\boldsymbol{r}$ between a certain two points in the real space of the scattering substance is subjected to parallel displacements into every position in all space, the total of the products of the densities $\rho(\boldsymbol{r})$ at the two ends of the vector is $Q(\boldsymbol{r})$. Thus if there are atoms at two points in space separated by a vector corresponding in magnitude and direction to $\boldsymbol{r}$, the value of $Q(\boldsymbol{r})$ will be large. Otherwise the value of $Q(\boldsymbol{r})$ for this $\boldsymbol{r}$ will be zero. $Q(\boldsymbol{r})$ therefore seems to be geometrically of the same nature as the density distribution functions of Eqs. 2.26, 2.33 and 6.74. This correspondence will be discussed later. If $\rho(\boldsymbol{r})$ is the electron density of an infinitely large crystal, $Q(\boldsymbol{r})$ is known as the Patterson function (usually written $P(\boldsymbol{r})$). The value of $Q(\boldsymbol{r})$ is large if there are atoms at both ends of the vector $\boldsymbol{r}$, and this important function assists materially in structural analysis by determining the vectors between the atoms in the crystal. Thus,

$$\begin{aligned}\rho(\boldsymbol{r}) * \rho(\bar{\boldsymbol{r}}) &= \int I(\boldsymbol{S})\exp\{2\pi i(\boldsymbol{S}\cdot\boldsymbol{r})\}\mathrm{d}v_s \\ &= P(\boldsymbol{r}) \text{ (the Patterson function in the case of crystals, } \textit{cf.} \text{ Eq. 11.41, Section 11.2.5)} \\ &= Q(\boldsymbol{r}) \text{ (general case)}\end{aligned} \tag{5.10}$$

These functions are obtained by Fourier transformation of the intensity distribution of the diffracted X-rays. The inverse transform is

$$I(\boldsymbol{S}) = \int Q(\boldsymbol{r})\exp\{-2\pi i(\boldsymbol{S}\cdot\boldsymbol{r})\}\mathrm{d}v_r \tag{5.11}$$

so that if the self convolution $Q(\boldsymbol{r})$ of the electron densities in a substance is known, the X-ray diffraction intensity is given by the Fourier transform of $Q(\boldsymbol{r})$. This is therefore an important equation.†

We shall now use the above Fourier transform and convolution theorems to derive a number of factors involved in X-ray analyses. (Fourier transformation of helical molecules is discussed in Section 11.4.)

---

† We have so far put forward Eq. 5.1 as the most convenient starting point for deriving X-ray intensities from the wave amplitude. What we fmd from experimental measurements are, however, not the wave amplitudes, but the intensity, and it is impossible to isolate the effect of phase from the amplitudes. Therefore, when we are seeking to determine structures on the basis of diffraction patterns it is safer to use Eq. 5.11.

5.2.2 Shape factor for the scattering body

The integrations in the equations beginning with Eq. 5.1 should in principle be carried out over all real space or reciprocal space. In X-ray diffraction experiments, however, even if the specimen is large enough to enable an approximation to this condition, only the scattering from a limited region is in fact observed. The following procedure minimizes the attendant difficulties.

The electron density distribution $\rho(\boldsymbol{r})$ in a particle of matter scattering X-rays, or in the case of a large specimen in the entire volume v within the X-ray beam, is expressed in terms of the electron density distribution $\rho_\infty(\boldsymbol{r})$ for the unbounded body as follows.

$$\rho(\boldsymbol{r}) = \rho_\infty(\boldsymbol{r}) \cdot \sigma(\boldsymbol{r}) \tag{5.12}$$

In this equation, the function $\sigma(\boldsymbol{r})$, which is known as the shape function, always takes the value unity when $\boldsymbol{r}$ lies within v, and is zero for all $\boldsymbol{r}$ outside v. On substitution of Eq. 5.12 in Eq. 5.1, by the convolution theorem, convolution of the Fourier transform $S(\boldsymbol{S})$ of $\sigma(\boldsymbol{r})$ and the fourier transform $A_\infty(\boldsymbol{S})$ of $\rho_\infty(\boldsymbol{r})$ gives the following equation.

$$A(\boldsymbol{S}) = A_\infty(\boldsymbol{S}) * S(\boldsymbol{S}) \tag{5.13}$$

If the scattering matter is represented as an infinite periodic arrangement similar to the lattice points of a crystal, then since $A_\infty(\boldsymbol{S})$ is the Fourier transform of the spatial distribution, it, too, is a periodic function with very narrow peaks, like the Laue function L in Eqs. 2.43 and 2.45. This is shown diagrammatically in Fig. 5.15(a) and (d). The convolution of $A_\infty(\boldsymbol{S})$ with $S(\boldsymbol{S})$ thus brings $S = 0$ in $S(\boldsymbol{S})$ to the positions of all the peaks (including the peaks with $S = 0$) of $A_\infty(\boldsymbol{S})$, as in Fig. 5.15(g). The width of the X-ray beam is usually large enough to ensure that the breadth of $S(\boldsymbol{S})$ is very small, and so there is seldom any practical necessity to take Eq. 5.13 into account when analyzing the structures of single crystals. Under these conditions $|S(\boldsymbol{S})|^2$ produces an effect only at very small values of 2θ, the so-called "form scattering" of the sample. On the other hand, in cases where the crystals are very small, as in solid high polymers and metals, the volumes v of the crystals themselves that are responsible for the interference effects are small, irrespective of the width of the X-ray beam, and $S(\boldsymbol{S})$ is found to have an appreciable broadening. This is seen in the broadening of each diffraction spot, and around the central spot formed by the incident beam (the small-angle scattering).

Where the scattering body is an assembly of particles, if $\rho(\boldsymbol{r})$ is a function having a fixed average density ρ_1 only inside the particles and a density ρ_0 outside the particles (which corresponds to the case of a single particle in space in small-angle scattering calculations), the Fourier transform $A_\infty(\boldsymbol{S})$ of ρ_0 over all space again has a very small peak like a point function $\delta(\boldsymbol{r})$ but now only at $\boldsymbol{S} = 0$. Its convolution with $S(\boldsymbol{S})$ is thus $S(\boldsymbol{S})$ displaced to the origin on $\boldsymbol{S} = 0$. $|S(\boldsymbol{S})|^2$ is therefore in itself a measure of the intensity distribution of the central small-angle scattering, which only depends on the shape (form) of the sample and, hence, is called form scattering (See text accompanying Eq. 6.1). To grasp the general application of this concept, let us consider the calculation of the diffraction intensity for a system of particles having an average electron density ρ_1 in a medium (*e.g.* in a solution) having an average density ρ_0. If we consider the density ρ_0 as being continuous over all space throughout the system, within which particles of density $\rho_1 - \rho_0$ float and if $\sigma_1(\boldsymbol{r}) = 1$ inside all particles and zero outside, the density distribution of the system is given by

$\rho_0 + (\rho_1 - \rho_0)\sigma(\boldsymbol{r})$. From the Fourier transform, the amplitude and intensity of the small-angle scattering are

$$A(\boldsymbol{S}) = \{\rho_0\delta(\boldsymbol{S}) + (\rho_1 - \rho_0)S_1(\boldsymbol{S})\} * S(\boldsymbol{S}) \tag{5.14}$$

The first term, like the Dirac point function $\delta(\boldsymbol{r})$, is usually unobservable since it occurs at the small angle 2θ, and it is called extremely form scattering:

$$I_0(\boldsymbol{S}) = \rho^2 \mid S(\boldsymbol{S}) \mid^2 \tag{5.14a}$$

The second term of Eq. 5.14 remains observable however. Assuming that the particles are small compared with the shape of the whole sample, one obtains:

$$I(\boldsymbol{S}) = I_0(\boldsymbol{S}) + (\rho_1 - \rho_0)^2 \mid S_1(\boldsymbol{S}) \mid^2 \tag{5.15}$$

It is evident that this intensity is proportional to $\Delta\rho^2$, where $\Delta\rho = \rho_1 - \rho_0$; we have thus verified the statement, made at the end of Section 6.2.2, concerning the influence of $\Delta\rho$ on the scattering intensity.

We shall now deal briefly with the self convolution of $\sigma_1(\boldsymbol{r})$, *i.e.*

$$\sigma_1(\boldsymbol{r}) * \sigma_1(\boldsymbol{r}) = Q_s(\boldsymbol{r}) \tag{5.16}$$

This function has a central peak at $\boldsymbol{r} = 0$ consisting of the self-convolution of the shape function σ_k of the N particles in the samples. If the particles have a Gaussian distribution, the particle distribution function $P(\boldsymbol{r})$ (see Section 2.5) practically = 1 for $r > 2R$ and, hence

$$Q_s(\mathrm{r}) = \sum_{k=1}^{N} \sigma_k(\mathrm{r}) * \sigma_k(\bar{\mathrm{r}}) = N < \sigma_k(\mathrm{r}) * \sigma_k(\bar{\mathrm{r}}) > \tag{5.16a}$$

By Fourier transformation Q_s, like $Q(\boldsymbol{r})$, again gives a diffraction intensity function that depends only on the number average self-convolution of the shape function $\sigma_k(\boldsymbol{r})$ of the particles. Applying Eq. 5.8 we obtain

$$I_s(\boldsymbol{S}) = \int_0^\infty Q_s(\boldsymbol{r}) \exp\{2\pi i(\boldsymbol{S}\cdot\boldsymbol{r})\} \mathrm{d}v_r$$

$$I(\boldsymbol{S}) = I_0(\boldsymbol{S}) + \Delta\rho^2 N < S_k(\boldsymbol{S}) S_k * (\boldsymbol{S}) > = I_0(\boldsymbol{S}) + \Delta\rho^2 N < \mid S_k(\boldsymbol{S}) \mid^2 > \tag{5.17}$$

From Eq. 5.13

$$A(\boldsymbol{S}) = A_\infty(\boldsymbol{S}) * S(\boldsymbol{S}), \qquad A(\boldsymbol{S})A^*(\boldsymbol{S}) = \mid A_\infty(\boldsymbol{S}) \mid^2 * \mid S(\boldsymbol{S}) \mid^2 = I(\boldsymbol{S}) \tag{5.18}$$

It is evident that Eq. 5.18 contains terms which correspond to the intensity $I_s(\boldsymbol{S})$ and the form scattering ($\mid S(\boldsymbol{S}) \mid^2$). The two together give the distribution of the small-angle scattering which corresponds to the shape of the particle and the shape of the whole sample, which is generally unobservable.

Finally, we shall explain the geometrical significance of $Q_s(\boldsymbol{r})$ utilizing Fig. 5.8 (*cf.* Eq. 5.9)

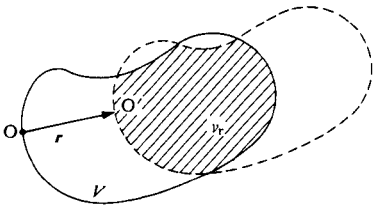

Fig. 5.8 Particle of volume V undergoing displacement $\boldsymbol{r}$ (see text for meaning of $Q_s(\boldsymbol{r})$ in this context).

Figure 5.8 shows the shape of a particle (continuous line) whose volume is V. If the particle as a whole undergoes a parallel displacement in the direction of an arbitrary vector $\boldsymbol{r}$ from a fixed point O in the particle to bring O into coincidence with the other end of the vector $\boldsymbol{r}$, its new position will be as shown by the broken line. The shape bounded by the broken line is called a ghost of the original particle (the scattering body). The value of the self convolution $Q_s(\boldsymbol{r})$ of the shape function of the particle for a given $\boldsymbol{r}$ is the sum of only those terms for which the product of the ends of $\boldsymbol{r}$ is $1 \times 1 = 1$ for parallel displacement of $\boldsymbol{r}$ to all possible positions in the original particle. If the volume common to the original particle and the ghost is v_r, as shown in the diagram, and if the ratio of this part to the total volume is $V(\boldsymbol{r})$,

$$Q_s(\boldsymbol{r}) = v_r = VV(\boldsymbol{r}) \tag{5.19}$$

This is a three-dimensional analogue of the situation in Fig. 5.7.

5.2.3 Scattering factor of atoms undergoing thermal vibrations in a crystal

As was shown in Eq. 2.15, the scattering factor of an atom at rest in a crystal lattice is given by the Fourier transform of its electron density $\rho_0(\boldsymbol{r})$ in the theoretical position. This is the atomic scattering factor given by Table 3 of the Appendix. In reality, however, the atoms in a crystal are not at rest, but undergo thermal vibrations about their respective "rest" positions. The displacements of the various atoms from their mean positions at a given instant must therefore be taken into account in calculating the structure factor $F(hkl)$.

To simplify the calculation it is assumed that each atom vibrates with isotropic harmonic motion, and that if the displacements from their rest positions of all the crystallographically equivalent atoms at a given moment are the same as that of any single vibrating atom, the electron densities of the individual atoms would be expressed by the average of a Gaussian distribution function having a mean square displacement $\overline{u}^2$. Thus if the function $\rho_0(\boldsymbol{r})$ is averaged for all positions of $\boldsymbol{r}$ by a function $\rho_1(\boldsymbol{r})$, the effective electron density $\rho_{at}(\boldsymbol{r})$ is the convolution $\rho_0 * \rho_1$. Taking ρ_1 as a Gaussian function, therefore, we find

$$\rho_{at}(\boldsymbol{r}) = \rho_0(\boldsymbol{r}) * \rho_1(\boldsymbol{r}), \qquad \rho_1(\boldsymbol{r}) = (2\pi\overline{u}^2)^{-3/2} \exp(-r^2/2\overline{u}^2) \tag{5.20}$$

The effective atomic scattering factor f_{at} is therefore the Fourier transform of $\rho_{at}(\boldsymbol{r})$, and application of Eq. 5.8 gives

$$f_{at}(S)=\int \rho_0(r) * \rho_1(r)dv_r = f(S)\exp(-2\pi^2\overline{u}^2S^2)$$

$$= f(\boldsymbol{S})\exp\{-8\pi^2\overline{u}^2(\sin^2\theta)/\lambda^2\}$$

$$D = \exp\{-8\pi^2\overline{u}^2(\sin^2\theta)/\lambda^2\} = \exp\{-B(\sin^2\theta)/\lambda^2\} \quad (5.21)$$

In the above expressions, f, is the Fourier transform of ρ_0, *i.e.* the scattering factor of the atom at rest. D is known as the Debye factor and B is called the temperature factor. In many cases the thermal motions of atoms are not isotropic, and assuring the thermal motion of atoms to be ellipsoidal the anisotropic thermal parameters are used as the better approximation. These are important factors in X-ray analyses, and their practical use will be shown later (Eqs. 11.34 and 11.36 (a, b)).

5.2.4 Optical experiments on Fourier transforms

The Fourier transformations in Eqs. 5.2, 5.6, 5.9, and 5.11, and their inverse transformations, can only be performed numerically or analytically for a given function if the form is already known. If the form is not given, Eq. 5.2 cannot be calculated mathematically. However, Eq. 5.1 (Eq. 2.13), which is of the same form as Eq. 5.2, shows that the amplitude of the resultant diffracted wave is given combination of the phase-dependent contributions from every element of the structure. Therefore, even if the mathematical form of the electron density function, $\rho(\boldsymbol{r})$, of a substance is unknown, it may still be possible to construct a model structure which will embody suspected characteristic features of the substance. Comparison of the diffraction pattern from such a model structure with that from the substance itself can provide a means of evaluating the tentative structure. It is impossible to construct prepared structures of the same order of magnitude as atoms themselves; the scale is usually some tens of thousands of times greater. The model may consist of a two-dimensional array of black dots or holes marked on film or glass, and the scale multiplication is such that visible light can be used to produce the diffraction effects. The Fourier transform in this sense is effectively performed by so-called optical inversion. Eq. 5.1 is, of course, equally valid for all forms of wave motion, including X-rays, visible light, and electron beams. Diffraction experiments with atomic models using visible light (*e.g.* the sodium D line doublet) are often useful for checking the validity of structures of great complexity, such as those involved in the detailed investigation of fiber paracrystals. Examples where such light diffraction patterns have been employed are given in Fig. 5.9,[3] and 5.13.[4] The reader is referred to the various experiments which Hosemann has performed in this connection.[3]

The experimental arrangements used and examples of their application are shown in Fig. 5.9. The upper diagrams of Fig. 5.9(a) and (b) show optical systems for Fourier transforms and convolutions (including self convolutions), respectively. Fig. 5.9(a) includes the model of the lattice function $\rho(\boldsymbol{r})$ to be transformed, and its transform $A(\boldsymbol{S})$ is recorded photographically as the intensity $|A(\boldsymbol{S})|^2$, giving the Fraunhofer diffraction pattern shown. In Fig. 5.9(b), if the second model differs from the first, the convolution of the two is obtained. If, however, both models are the same, which is the case illustrated, the self convolution of the model is obtained. This is the means by which $\rho(\boldsymbol{r}) * \rho(\overline{\boldsymbol{r}})$, *i.e.* $Q(\boldsymbol{r})$, can be determined by visible light diffraction.

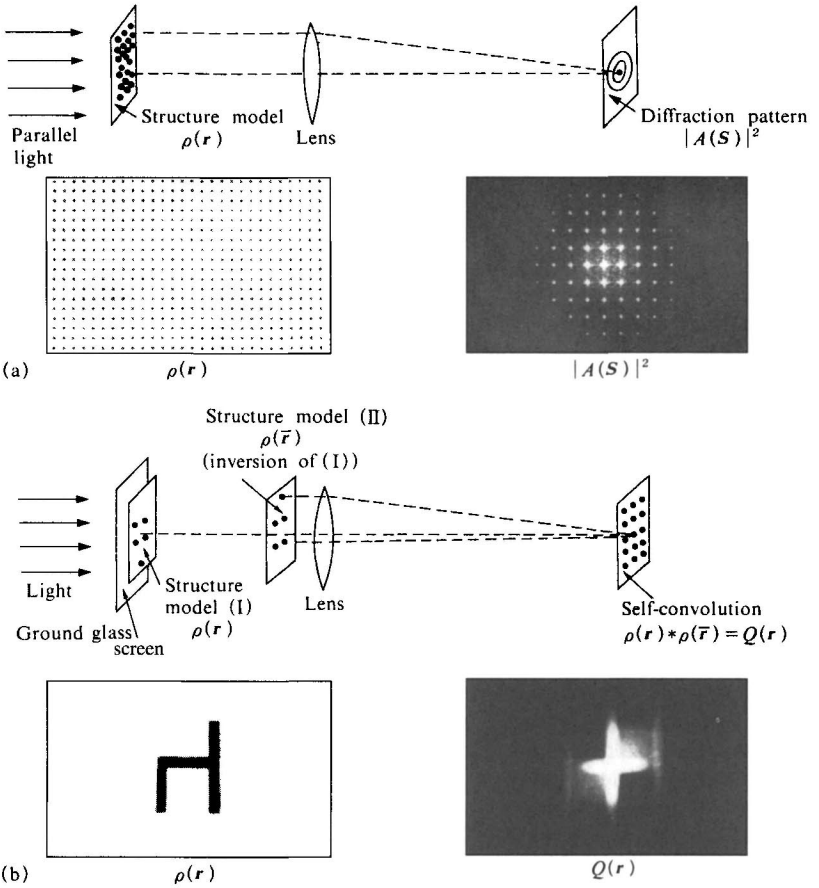

Fig. 5.9 Optical methods for Fourier transformations and convolutions.[3,4)]
(a) Fourier transformation. (b) Convolution (and self-convolution).
[Reproduced with permission from R. Hosemann, *Polymer*, **3**, 349, IPC Business Press (1962)]

5.3 Diffraction of X-Rays by Paracrystals†

For diffraction from a crystal, since the unit cells are arranged in a regular manner in accordance with Eq. 2.37, the phases of their scattering amplitude A_{cell} can be combined as shown in Eq. 2.38. For paracrystals, on the other hand, the positions of the lattice points can be expressed only as a statistical average, as was mentioned earlier. It is therefore necessary to find some adequate means of representing the positions of the lattice points, just

† after Hosemann[3,4)]

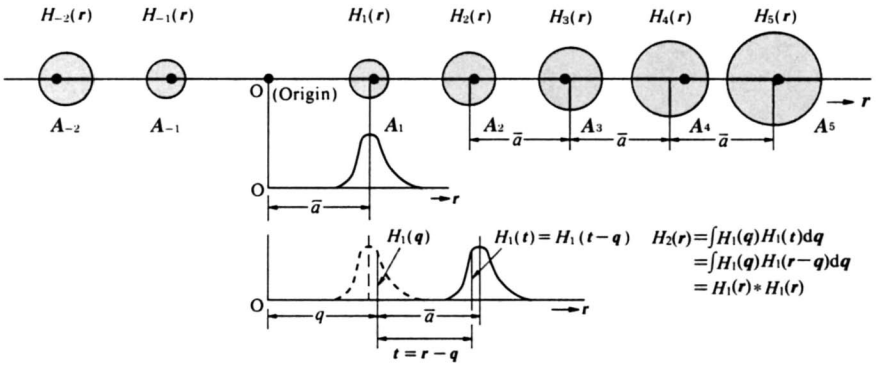

Fig. 5.10 Diagram showing the distribution of lattice points in a linear paracrystal.

as Eq. 2.37 does for crystals, and of combining their phases to find the diffraction due to the paracrystalline lattice. We first consider the paracrystal as a one-dimensional system having significant extension only in the $\boldsymbol{a}$ direction (Fig. 5.10).

5.3.1 Statistical representation of paracrystalline lattice points and the derivation of their function $Q(r)$

Let the lattice points in the $\boldsymbol{a}$ direction be A_1, A_2, etc., where A_1 is the nearest neighbor to some arbitrary origin, O. If the probability that A_1 be located by a vector $\boldsymbol{q}$ from the origin is $H_1(\boldsymbol{q})$, then the probability that A_2 is located by an independent vector $\boldsymbol{t}$ from the end of $\boldsymbol{q}$ will be $H_1(\boldsymbol{q}) \cdot H_1(\boldsymbol{t})$. The total probability, $H_2(\boldsymbol{r})$, that A_2 (the next nearest neighbor) will lie at the end of a single direct vector $\boldsymbol{r} = \boldsymbol{q} + \boldsymbol{t}$ from the origin is not, however, the product of two individual probabilities $H_1(\boldsymbol{q})$ and $H_1(\boldsymbol{t})$ if we assume that there is no statistical correlation between the individual $\boldsymbol{q}$ and $\boldsymbol{t}$ vectors. Since we are interested in the probability for a certain $\boldsymbol{r}$, whatever the value of $\boldsymbol{q}$ we have to integrate overall $\boldsymbol{q}$ for a fixed $\boldsymbol{r} = \boldsymbol{q} + \boldsymbol{t}$. Hence $\boldsymbol{t} = \boldsymbol{r} - \boldsymbol{q}$ and we finally obtain

$$H_2(\boldsymbol{r}) = \int H_1(\boldsymbol{q}) H_1(\boldsymbol{r}-\boldsymbol{q}) \mathrm{d}q = H_1(\boldsymbol{r}) * H_1(\boldsymbol{r}) \tag{5.22}$$

which is a convolution of $H_1(\boldsymbol{r})$ with $H_1(\boldsymbol{r})$ (*cf.* Eq. 5.6) and, in general, the probability fo the nth lattice point is

$$H_n = H_1 * H_1 * \cdots * H_1 \text{ (the } (n-1) \text{ fold convolution of } H_1) \tag{5.23}$$

$H_n(\boldsymbol{r})$ is normalized as unity, and $H_{-n}(\boldsymbol{r}) = H_n(-\boldsymbol{r})$, with $\int \boldsymbol{r} H_n(\boldsymbol{r}) \mathrm{d}r = n\bar{\boldsymbol{a}}$.

Let us now consider the extension of this treatment to three dimensions. In Fig. 5.11 the three points A_1, A_2, and A_3 are located by vectors $\boldsymbol{a}_1$, $\boldsymbol{a}_2$, and $\boldsymbol{a}_3$, corresponding to directions $\boldsymbol{a}$, $\boldsymbol{b}$, and $\boldsymbol{c}$ in an ideal lattice. The "nearest neighbor" probabilities in the three directions (corresponding to H_1 along $\boldsymbol{a}$ in the preceding discussion) may be written H_{100}, H_{010}, and H_{001} respectively, where $H_{pqr}(\boldsymbol{r})$ denotes the probability that the vector $\boldsymbol{r}$ from the origin will locate the point which is the pth in the $\boldsymbol{a}_1$ direction, the qth in the $\boldsymbol{a}_2$ direction, and the rth in the $\boldsymbol{a}_3$ direction. This probability can be expressed in terms of the $(p-1)$ fold convolution of H_{100}, the $(q-1)$ fold convolution of H_{010}, and the $(r-1)$ fold convolution of H_{001},

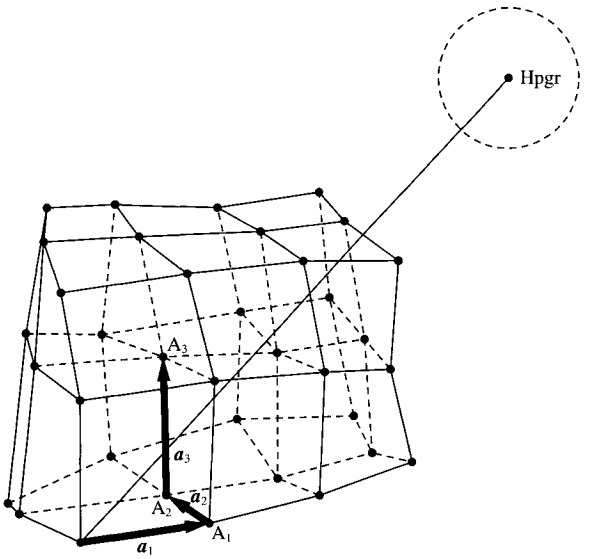

Fig. 5.11 Paracrystalline lattice in three dimensions (*cf.* Fig. 5.6(b_2')).

with an extra normalizing term if the probability at the origin is taken as unity. Thus

$$H_{pqr} = H_{000} * \underbrace{H_{100} * H_{100} \cdots * H_{100}}_{(p-1)\text{fold}} * \underbrace{H_{010} * \cdots * H_{010}}_{(q-1)\text{fold}} * \underbrace{H_{001} * \cdots * H_{001}}_{(r-1)\text{fold}} \tag{5.24}$$

H_{000} is a point function having a definite value only at the origin. Eq. 5.24 expresses the probability that a lattice point (pqr) will exist at a point displaced by the appropriate number of multiples (p, q, and r) of the average lengths $\bar{a}_1$, $\bar{a}_2$, and $\bar{a}_3$ of the sides of the cell from an origin at some arbitrary lattice point.

A lattice point (pqr) can be reached by several independent paths, depending upon the directions taken from point to point along the route through the paracrystal. The H_{pqr} of Eq. 5.24 is therefore but one element in the total probability, which must be summed for all possible paths from an arbitrary lattice-point origin to the point (pqr) located by vector $\boldsymbol{r}$, *i.e.*

$$\sum_p \sum_q \sum_r H_{pqr} = \sum_{p=-\infty}^{\infty} H_{p00} * \sum_{q=-\infty}^{\infty} H_{0q0} * \sum_{r=-\infty}^{\infty} H_{00r} = z(\boldsymbol{r})_{pqr} \tag{5.25}$$

5.3.2 Lattice factor and diffraction intensity for a paracrystal

Having derived a statistical distribution, $z(\boldsymbol{r})$, for the distance between lattice points in a paracrystalline lattice, we proceed to use it to calculate the diffraction intensity.

Let the Fourier transform of $H_k(\boldsymbol{r})$ be $\mathcal{F}_k(\boldsymbol{S})$, where H_k replaces H_{pqr} in the preceding analysis for (pqr) equal to (100), (010), or (001). We shall now calculate the scattering intensity for the X-ray scattering from all the lattice points of a paracrystal, taking the scattering factor A_{cell} of the unit cells as unity and considering only the intensity due to the lattice structure.

The quantity $z(\boldsymbol{r})$ is just the probability function $P(\boldsymbol{r})/v$ of Section 2.5, no longer spherically symmetric but with paracrystalline lattice character. It may be regarded as the probability distribution for the presence of lattice points of the same unit density at both ends of a given vector $\boldsymbol{r}$. This is simply the self convolution of a density distribution $\rho(\boldsymbol{r})$, *i.e.* $Q(\boldsymbol{r})$, (*cf.* Eq. 5.9) having point function $\delta(\boldsymbol{r})$ only at positions occupied by lattice points. The X-ray diffraction intensity due to the paracrystalline lattice structure itself is therefore given directly by the Fourier transform of $z(\boldsymbol{r})$, according to Eq. 5.11. Let the Fourier transform of $z(\boldsymbol{r})$ for the k direction ($k=(100)$, (010), or (001)) be $K_k(\boldsymbol{S})$. If M is the number of unit cells along each axis in the paracrystal, then$\mathscr{F}$

$$K_k(\boldsymbol{S})=\sum_{p=0}^{\infty}(\mathscr{F}_k{}^{p}+\mathscr{F}_k{}^{*p})-1=\lim_{M\to\infty}2\,\mathrm{Re}\left(\frac{1-\mathscr{F}_k{}^{M+1}}{1-\mathscr{F}_k}\right)-1$$

$$=\lim_{M\to\infty}\mathrm{Re}\left(\frac{2-2\mathscr{F}_k{}^{M+1}-1+\mathscr{F}_k}{1-\mathscr{F}_k}\right)=\mathrm{Re}\left(\frac{1+\mathscr{F}_k}{1-\mathscr{F}_k}\right)+\lim_{M\to\infty}\mathrm{Re}\left(\frac{-2\mathscr{F}_k{}^{M+1}}{1-\mathscr{F}_k}\right) \tag{5.26}$$

$\mathscr{F}_k{}^*$ is the Fourier transform of H_k for points on the negative side of the origin, and is the complex conjugate function of that for points on the positive side, $\mathscr{F}_k$. Re denotes the real part. If we let the second term in Eq. 5.26 be $K(0)$, then

$$K(0)=-2\lim_{M\to\infty}\frac{\mathrm{Re}(1-\mathscr{F}_k{}^{*})\cdot\mathscr{F}_k{}^{M+1}}{|1-\mathscr{F}_k|^2} \tag{5.27}$$

The complex $\mathscr{F}_k$ may be represented by modulus and phase, thus

$$\mathscr{F}_k(\boldsymbol{S})=|\,\mathscr{F}_k(\boldsymbol{S})\,|\exp\{-2\pi i(\bar{\boldsymbol{a}}_k\cdot\boldsymbol{S})\},$$

$$\mathscr{F}_k{}^{*}(\boldsymbol{S})=|\,\mathscr{F}_k(\boldsymbol{S})\,|\exp\{2\pi i(\bar{\boldsymbol{a}}_k\cdot\boldsymbol{S})\},\ \text{and}$$

$$\bar{\boldsymbol{a}}_k=\int r H_k(r)\,\mathrm{d}v \tag{5.28}$$

if $H_k(r)$ has a center of symmetry.
We obtain

$$K(0)=\lim_{M\to\infty}|\mathscr{F}_k|^M\,\frac{\sin\pi(2M+1)(\bar{\boldsymbol{a}}_k\cdot\boldsymbol{S})}{\sin\pi(\bar{\boldsymbol{a}}_k\cdot\boldsymbol{S})} \tag{5.29}$$

$$K_k(\boldsymbol{S})-K(0)=\mathrm{Re}\,\frac{1+\mathscr{F}_k}{1-\mathscr{F}_k} \tag{5.30}$$

The form of the second term of $K(0)$ in Eq. 5.29 is evidently similar to the form of the Laue function (Eq. 2.38). The presence of the $|\,\mathscr{F}_k\,|^M$ factor (with $|\,\mathscr{F}_k\,|<1$), however, ensures that $K(0)$ approximates to a peak function having significant values only for a small range of $\boldsymbol{S}$ centered about $\boldsymbol{S}=0$. Eq. 5.30, from which the central peak of $K(\boldsymbol{S})$ has been subtracted, gives the most important part of the diffuse pattern which characterizes second and higher order diffraction from paracrystals. In fact, when M is not infinitely large, but is a finite, small number, we find a "broadening" similar to that for the Laue function in Section 2.9.2. This will be discussed further at a later stage. From Eq. 5.30,

$$K_k(\boldsymbol{S})-K(0)=\frac{1-|\mathscr{F}_k|^2}{1+|\mathscr{F}_k|^2-2\,|\mathscr{F}_k|\cos 2\pi(\bar{\boldsymbol{a}}_k\cdot\boldsymbol{S})} \tag{5.31}$$

Since the principal term on the left-hand side is $K_k(\boldsymbol{S})$, we obtain from Eq. 5.31

$$K_k(\boldsymbol{S})(\max) = \frac{1+|\mathscr{F}_k|}{1-|\mathscr{F}_k|} \quad (\text{if } \bar{\boldsymbol{a}}_k \cdot \boldsymbol{b} = h_k) \tag{5.32}$$

$$K_k(\boldsymbol{S})(\min) = \frac{1+|\mathscr{F}_k|}{1-|\mathscr{F}_k|} \quad (\text{if } \bar{\boldsymbol{a}}_k \cdot \boldsymbol{b} = h_k + \frac{1}{2}) \tag{5.33}$$

where h_k is an integer. These are the basic equations giving the maximum and minimum values of the intensity of the diffuse diffraction pattern from a paracrystal. They are a generalization of the Laue conditions, Eq. 2.39. Gathering together the expressions for the three dimensions, one can prove that the result is

$$Z(\boldsymbol{S}) = K_1 K_2 K_3 = \frac{1}{v}\delta(\boldsymbol{S}-0) + \prod_{k=1}^{3} \mathrm{Re}\frac{1+|\mathscr{F}_k|}{1-|\mathscr{F}_k|} \tag{5.34}$$

$\delta(\boldsymbol{S}-0)$ represents the term $K(0)$, which is a three-dimensional point function at $\boldsymbol{S}=0$, the suffixes 1, 2, and 3 refer to the three directions, and v is the average volume of the unit cell. Eq. 5.34 is the most important equation for the X-ray intensity for a substance having a paracrystalline structure. $Z(\boldsymbol{S})$ is called the paracrystalline lattice factor, and it corresponds to the Laue function for the ideal crystal. The diffraction maxima occur at the same positions as the diffraction spots for an ideal crystal, whereas the diffuseness of the diffraction peaks increases with the index of the diffraction (reflection) due to the contribution of the second term. The broadening also increases with increasing lattice distortion, and finally, for a given index, the intensity peaks merge indistinguishably with the background or with the peaks of the next higher index. This is schematically shown in Fig. 5.12. The right figures show, from top to bottom, square of the average unit cell scattering amplitude of an average net plane (say the $(h00)$ plane), $|<A_{\mathrm{cell}}(\boldsymbol{S})>|^2$, paracrystalline lattice factor, $Z(\boldsymbol{S})$, and intensity, $I(\boldsymbol{S}) = |<A_{\mathrm{cell}}(\boldsymbol{S})>|^2 \cdot Z(\boldsymbol{S})$. In the left those for an ideal crystal (Fig. 2.20) are shown again for comparison. This topic will be covered in a later section (*cf.* 13.6.3).

It should be noted that although several important equations were developed in terms of three dimensions, the treatment is basically one-dimensional in that it presumes no relationship between the dimensions. In the general case certain problems arise. Thus it was assumed at the beginning of this section that the "original ideal lattice" could be discerned. In the case of completely disordered amorphous substances, however, it is meaningless to speak of a vector in the $\boldsymbol{a}$, $\boldsymbol{b}$, or $\boldsymbol{c}$ directions, because the directions are indistinguishable in isotropic amorphous substances. The applicability of this method therefore depends upon the degree of distortion from the ideal lattice for a given single direction in the specimen, *e.g.* the direction of the molecular chains or a specified direction in the plane normal to the direction of the chains. A measure of the degree of distortion can be obtained by forming a weighted average of the probabilities H_k of finding displaced lattice points in the various directions. This average is taken over the whole of the specimen but, since H is very diffuse and small in value for the highest degree of distortion, it should be clear that the average will not be greatly affected by contributions from amorphous regions. Fig. 5.13[4] (p.102) gives a comparison between the theoretical value of H and experimental values. Fig. 5.13(a) shows H_{00} H_{10} and H_{01} for a paracrystalline lattice, and Fig. 5.13(b) shows the lattice point model constructed on this basis. Fig. 5.13(c) illustrates H for various lattice points as found by two-dimensional synthesis of the H values calculated from the model. Fig. 5.13(d) shows the optical diffraction pattern obtained in an actual experiment with this model; this diffraction pattern corresponds to the Fourier transform of the H of Fig. 5.13(b).

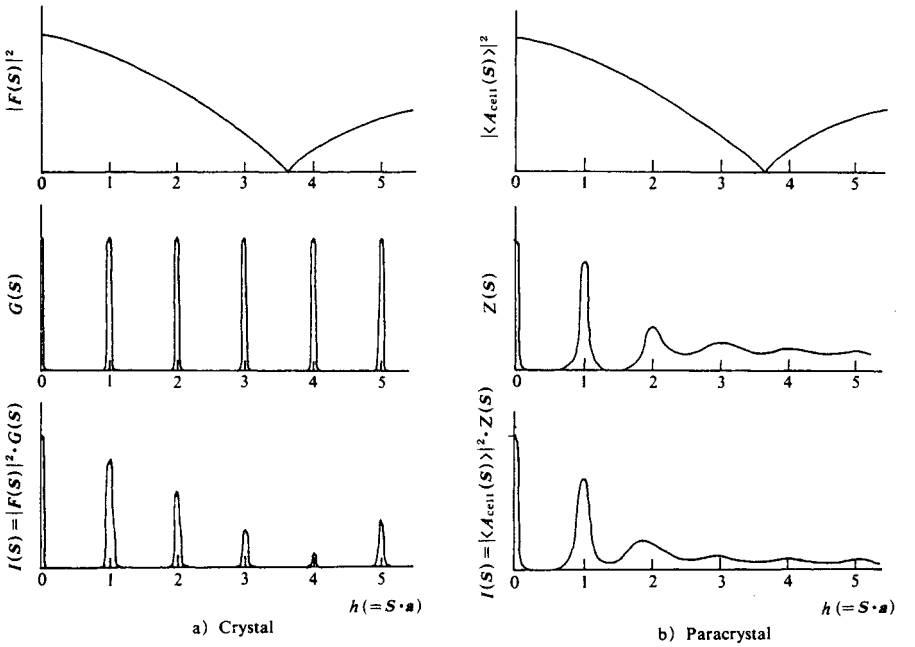

Fig. 5.12 A schematic comparison of diffraction intensities by crystal and paracrystal.
a) Crystal: (from top to bottom) Square of structure factor, $|F(S)|^2$; Laue function, $G(S)$; Intensity, $I(S)=|F(S)|^2\cdot G(S)$ [Reproduced with permission from R. D. B. Fraser, T. P. Mac Rae, *Conformations in Fibrous Proteins and Related Synthetic Polymers*, p.8, Academic Press (1973)]
b) Paracrystal: (from top to bottom) Square of average unit cell scattering amplitude, $|\langle A_{cell}(S)\rangle|^2$ (for simplicity, magnitude of $|\langle A_{cell}(S)\rangle|^2$ is taken the same as $|F(S)|^2$); Paracrystalline lattice factor $Z(S)$; Intensity, $I(S)=|\langle A_{cell}(S)\rangle|^2\cdot Z(S)$.

We have so far referred to H only as the probability of the presence of a lattice point, and no reference has been made to its actual form. In many paracrystalline substances, bearing in mind the physical causes of distortion in the crystal, it is often legitimate to choose a Gaussian-type function for the H that expresses the distribution. As shown in Fig. 5.14 (p.103),[4] therefore, if we take the $H_k(r)$ for the three principal directions of the orthogonally paracrystalline lattice cell ($k = 1$, 2, or 3) as a three-dimensional Gaussian function, it can be expressed in terms of a matrix T_{jk} consisting of nine elements of mean-square displacements from the regular lattice, $\Delta^2 r_{jk}$, in groups of three for each principal axis. The Fourier transform of H, when it takes the form of a one-dimensional Gaussian function is $\mathcal{F}_k(S)$, which is already given in Eq. 5.28, and in the equation

$$\mathcal{F}_k(S)=\exp\{-2\pi^2\,(S\cdot T_k\cdot S)\} \tag{5.35}$$

$$(S\cdot T_k\cdot S)=\sum_{kj} T_{jk}S_jS_k \tag{5.36}$$

$$T_{jk}=\begin{pmatrix}\Delta^2 r_{11} & \Delta^2 r_{12} & \Delta^2 r_{13}\\ \Delta^2 r_{21} & \Delta^2 r_{22} & \Delta^2 r_{23}\\ \Delta^2 r_{31} & \Delta^2 r_{32} & \Delta^2 r_{33}\end{pmatrix},\quad (\Delta^2 r_{jk}=\Delta^2 r_{kj}), \tag{5.37}$$

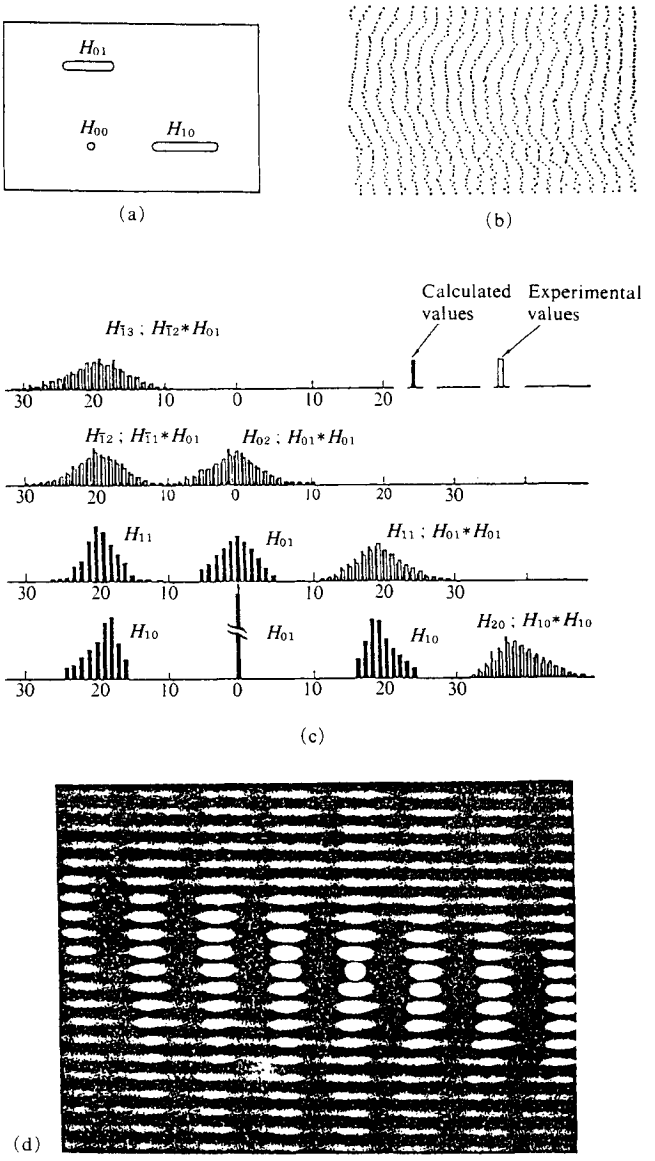

Fig. 5.13 A comparison between theoretical and experimental values of H.[4)]
(a) H_{00}, H_{01}, and H_{10} for a paracrystalline lattice; (b) The paracrystalline lattice model corresponding to (a); (c) Convolution values found from the diffraction pattern (d) and those calculated directly from the model; (d) Optical (Fraunhofer) diffraction pattern derived from this model (b).
[Reproduced with permission from R. Hosemann, S. N. Bagchi, *Direct Analysis of Diffraction by Matter*, pp.143, 144, 146, North-Holland Pub. (1962)]

(see Fig. 5.14). It should be noted that Eq. 5.35 is of exactly the same form as the Debye factor, D of Eq. 5.21.

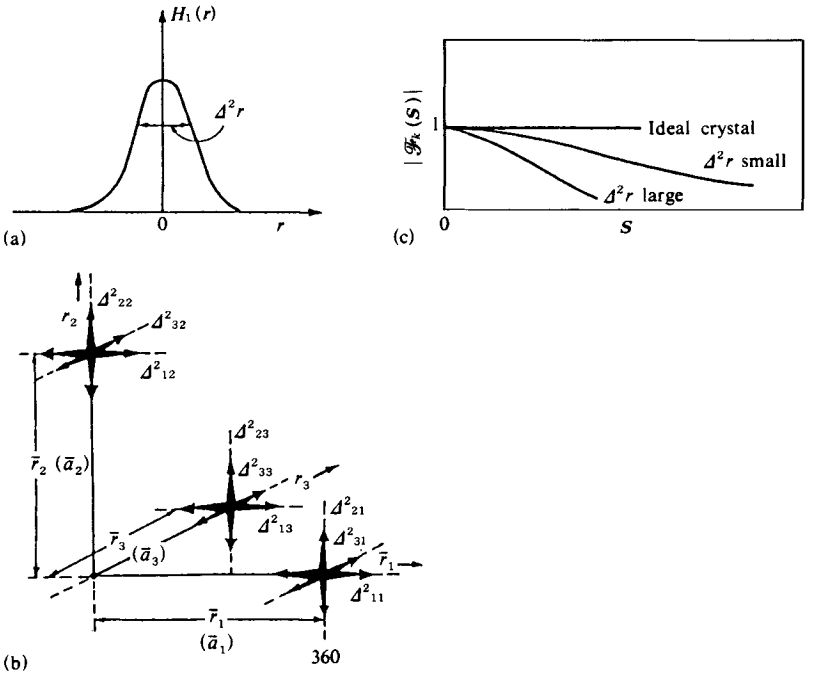

Fig. 5.14 Delineation of H, and its effect on $|\mathcal{F}_k|$ (see text, and also *cf.* Fig. 11.8 for Z).[4)]
(a) One-dimensional $H_1(r)$ (Gaussian, *cf.* Fig. 5.10 for the general case, unsymmetrical distribution);
(b) Tensor representation of the corresponding paracrystalline lattice distortion in the directions 1, 2, and 3 by means of the nine symmetrical matrix elements Δ_{11}^2, Δ_{22}^2, etc.; (c) $|\mathcal{F}_k(S)|$ vs. S for various degrees of distortion.
[Reproduced with permission from R. Hosemann, *Polymer*, **3**, 349, IPC Business Press (1962)]

This concludes the fundamental analysis of X-ray diffraction intensities for paracrystalline structures, and we can combine the results to obtain an equation for the X-ray diffraction intensity found in practice. A paracrystal differs from a normal crystal in that the unit cells are not all identical, so there is no unique A_{cell} which expresses the composite amplitude due to all the atoms in the unit cell. It is therefore necessary to use an averaged $<A_{\text{cell}}>$ over all unit cells. Taking the system as a dense array of cells having different structure factors, and applying the reasoning which gave Eqs. 2.30, 2.33, and 2.34, we can find the intensity with the aid of the $Z(S)$ obtained by the statistical method of this chapter for the distortion of the lattice period, thus:

$$I(S)=\bar{N}(<A_{cell}{}^2>-D_1^2<A_{cell}>^2)+\frac{1}{v}<A_{cell}>^2<D_1^2>^2(Z(S)*|S(S)|^2) \qquad (5.38)$$

D_1^2 is the distortion factor of the first kind, and is of the same form as Eq. 5.21. $\bar{N}$ is the total number of unit cells, and v is the average volume of one unit cell. $|S(S)|^2$ is the shape

factor of the domain of the paracrystalline lattice given in Eq. 5.17, or may be regarded as the contribution due to the shape of the coherent boundaries with shape factor $|S(\boldsymbol{S})|^2$ in a polyparacrystalline material (see Eq. 5.17).

5.4 Summary of the Relationship between Structure and X-Ray Diffraction Intensity

The description of the X-ray diffraction intensities due to material systems, except for very small bodies (see Chapter 6), has now been completed for practically all forms of atomic structures and for cases ranging from those in which the structural units are large to those consisting of very small domains. The methods of finding the X-ray diffraction intensities for the various systems (single molecules, gases, liquids, amorphous materials, paracrystals, crystals, and including the effect on the scattering from particles due to their shape factor) can be roughly divided into two basic procedures.

1) The first involves treating the smallest scattering units as the atoms and using the corresponding atomic scattering factor f to find the composite scattered amplitude from calculations using the phase differences due to the differing positions of the atoms.

2) The second involves finding the self-convolution $Q(\boldsymbol{r}) = \rho(\boldsymbol{r}) * \rho(-\boldsymbol{r})$ of the density distribution function of the system; the scattering intensities for the system are obtained by Fourier transformation of $Q(\boldsymbol{r})$.

Liquids and amorphous substances possess neither the complete long-range order of crystals, nor the partial long-range ordering of paracrystals, and it is not possible, therefore, to make unqualified use of a periodical lattice function like $z(\boldsymbol{r})$ (*cf.* Eq. 5.25). In calculations in these cases, $z(\boldsymbol{r})$ should be considered as expressing the short-range order. Here we omit the intermediate equations and cite only the results. Their form shows distinct similarities with the results obtained by the methods of Section 5.2 and by calculation of the diffraction intensities for paracrystals. The general form of the equations for liquids, amorphous substances, densely packed particle systems, etc., representing the scattering factors of the atoms or molecules of the liquid or amorphous substance or the scattering factors of the particles as $A(\boldsymbol{S})$, is as follows:

$$I(\boldsymbol{S}) = M[<|A^2(\boldsymbol{S})|> |S(\boldsymbol{S})|^2 + |<A(\boldsymbol{S})>|^2 \Phi(\boldsymbol{S}) * |S(\boldsymbol{S})|^2] \tag{5.39}$$

where

$$\Phi(\boldsymbol{S}) = 1 + \frac{1}{v_1}\int \{P(\rho) - 1\} \exp\{2\pi i(\Sigma \cdot \rho)\} \mathrm{d}v \tag{5.40}$$

For the individual case, the reader is referred to earlier sections (*cf.* Sections 2.5 – 2.8).

For crystals

$$I(\boldsymbol{S}) = \frac{1}{v}|F(\boldsymbol{S})|^2 \, G(\boldsymbol{S}) * |S(\boldsymbol{S})|^2 \tag{5.41}$$

For crystals containing distortions of the first kind we have

$$I(\boldsymbol{S}) = |F(\boldsymbol{S})|^2 \, [N(1 - D_1^2) + \frac{1}{v} \cdot D_1^2 G(\boldsymbol{S}) * |S(\boldsymbol{S})|^2] \quad \text{(Thermal motion)} \tag{5.42}$$

$$I(\boldsymbol{S}) = N[<|F(\boldsymbol{S})|^2> - |<F(\boldsymbol{S})>|^2] + \frac{1}{v}|<F(\boldsymbol{S})>^2 G(\boldsymbol{S}) * |S(\boldsymbol{S})|^2$$

(Mixed crystals) (5.43)

For paracrystals containing distortions of both the first and second kinds (distortion factor D_t) we have

$$I(\boldsymbol{S}) = N(<|A_{cell}|^2> - D_t^2 <A_{cell}>|^2) + \frac{1}{v}|<A_{cell}>|^2 D_t^2 Z(\boldsymbol{S}) * |S(\boldsymbol{S})|^2 \quad (5.44)$$

In the above equations, $G(\boldsymbol{S}) = L_1^2(N_1)L_2^2(N_2)L_3^2(N_3)$ is the Laue function, v_1 is the volume occupied by one particle (atom or molecule), v is the volume of a unit cell, M the total number of particles, and N the number of unit cells. Since the shape of the crystalline or paracrystalline single lattice is taken into consideration by the shape factor $|S(\boldsymbol{S})|^2$, the numbers N_1, N_2, and N_3 in the Laue function (*cf.* Eqs. 2.38 and 2.45) are infinitely large, and hence $G(\boldsymbol{S})$ has point-like peaks in the reciprocal lattice points.

1) For amorphous substances, the integral containing $P(\boldsymbol{r})$ is the Fourier transform of the statistical distribution of the distances of the scattering points, while for paracrystals and crystals, $Z(\boldsymbol{S})$ and $G(\boldsymbol{S})$ are the Fourier transforms of the statistical distribution of the distances of the lattice points. The similarity between Eqs. 5.43 and 5.44 is particularly obvious.

2) When the different phases of a substance (crystalline or paracrystalline, amorphous or liquid) are finely divided into very small regions, or in the case of fine particles, the small-angle scattering of X-rays to be discussed in Chapter 6 is quite appreciable because of the $|S(\boldsymbol{S})|^2$ factor (see Eq. 5.17). In the case of crystals or paracrystals, small-angle scattering is observed not only for $\boldsymbol{S} = 0$ (*i.e.* in the direction of the incident beam), but at each diffraction spot, owing to the convolution of the shape factor $|S(\boldsymbol{S})|^2$ of the lattices with $G(\boldsymbol{S})$ or $Z(\boldsymbol{S})$. For amorphous substances, liquid or solution it is observed only at the center spot.

3) When the crystals are small, broadening of $G(\boldsymbol{S})$ occurs in accordance with Fig. 2.16, and it should be understood that the resultant broadening of the diffraction spots will be further increased by convolution with the factor $|S(\boldsymbol{S})|^2$. The latter contribution, of course, is at its most intense in the direction of the incident beam.

Reference to Fig. 5.15 will clarify the above conclusions. It also illustrates the method in 2) above for calculating X-ray diffraction intensities.

Since direct Fourier transformation for a crystal of finite size (represented in one dimension in Fig. 5.15(c)) is impossible (*cf.* Section 5.2.2), the lattice function of the crystal with finite size is obtained by considering an infinitely large crystal (a) conjunction with a shape function $\sigma(\boldsymbol{r})$, (b). The self-convolution $Q(\boldsymbol{r})$ (e) of the lattice function (c) is the product of the two self-convolutions z and $Q_s(\boldsymbol{r})$ (in Fig. 5.15(e). The diffraction intensity is then found by Fourier transformation of $Q(\boldsymbol{r})$ (*i.e.* of $z(\boldsymbol{r}) \cdot Q_s(\boldsymbol{r})$). The result is the convolution (in (g)) of the individual Fourier transforms shown in diagram (f). The intensity distribution (g) can also be derived as the broadening of the Laue function due to the fact that in the case we are considering the crystals are finite with small numbers of unit cells, but here we have obtained it as the broadening of the shape function $|S(\boldsymbol{S})|^2$. The diagram shows that the small-angle scattering is not restricted to the center, but is associated with all the diffraction spots. In Fig. 5.15 $\mathcal{F}$ denotes a Fourier transform.

A similar analysis for paracrystals in Fig. 5.16 gives the intensity distribution shown in diagram Fig. 5.16(g). Although we are considering a paracrystal with infinite extension, the broadening of $z(\boldsymbol{r})$ increases with increase in the order of diffraction due to the distortion of the lattice, and the diffraction intensity also broadens out with increasing order number, as shown in Figs. 5.12 and 13.16. For finite crystals, therefore, this broadening will be further increased by convolution with the broadening of $|S(\boldsymbol{S})|^2$ (*cf.* Section 13.6).

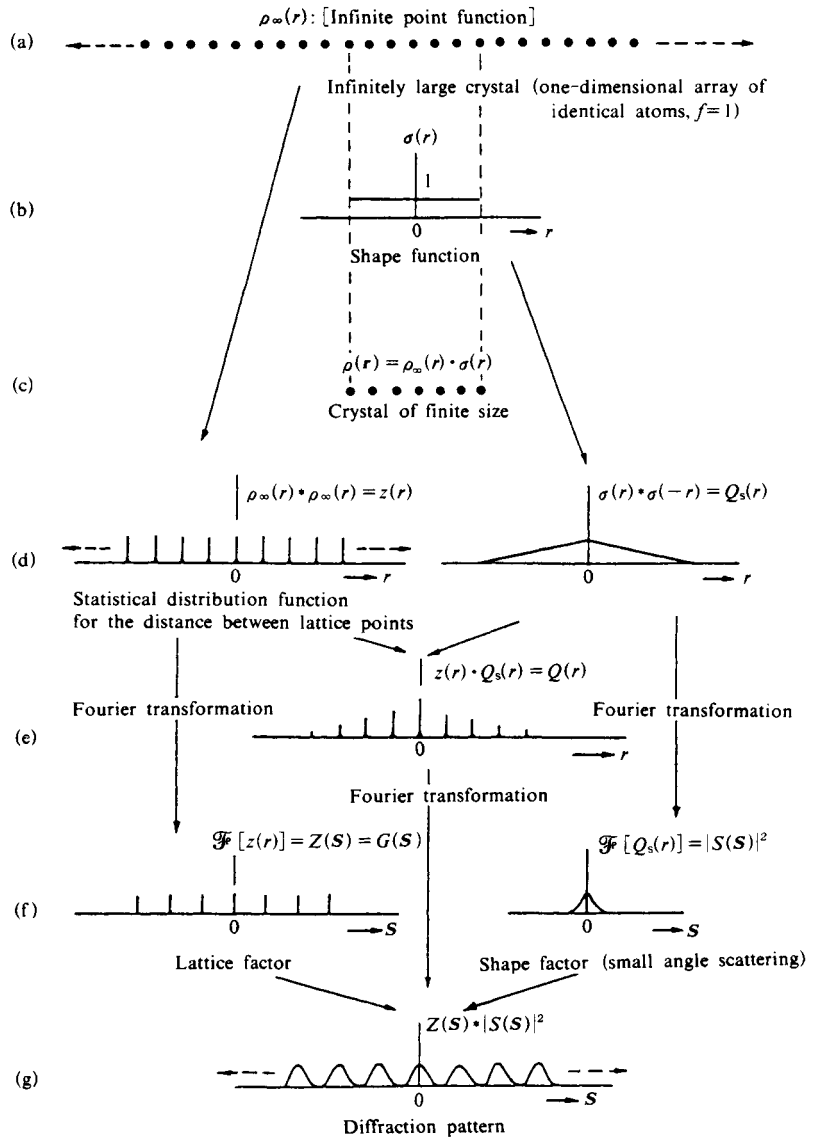

Fig. 5.15 Schematic representation of the steps involved in calculating the diffracted X-ray intensities (bounded crystals). Atomic scattering factors, f's are taken as unity. $\mathcal{F}$ denotes a Fourier transform.

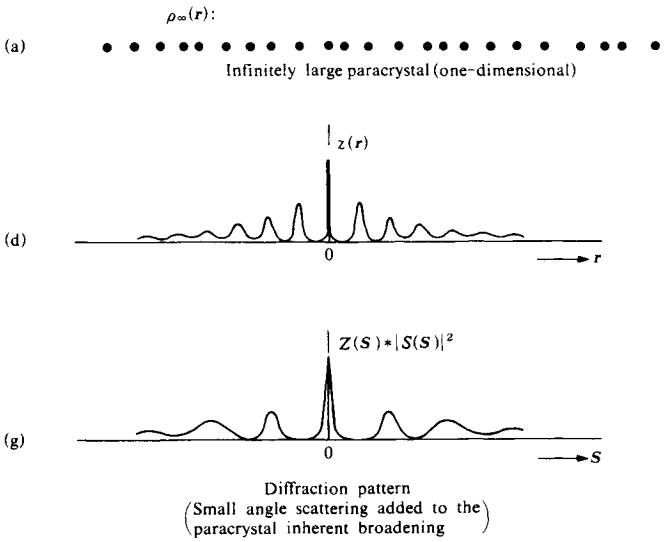

(Small-angle scattering added to the paracrystal inherent broadening)

Fig. 5.16 Schematic representation of the steps in calculating X-ray intensities (bounded paracrystals). Only those steps corresponding to (a), (d), and (g) in Fig. 5.15 are shown. Atomic scattering factors are taken as unity.

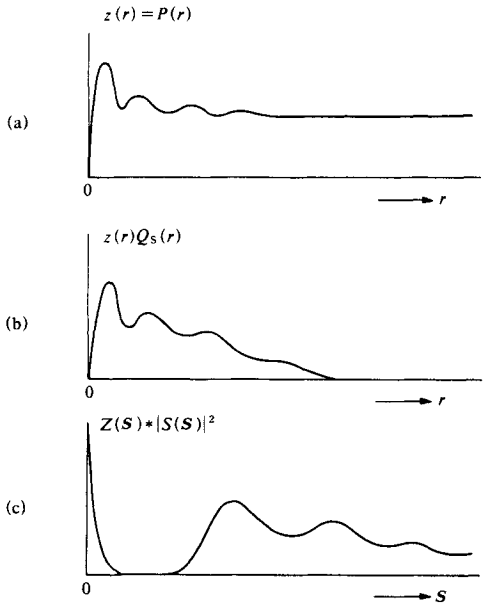

Fig. 5.17 Steps in calculating scattered X-ray intensities (amorphous substances).

The diffraction from a system of amorphous particles is simple, as is evident from Fig. 5.17. Attention has already been drawn to the fact that $Q(\boldsymbol{r})$ in this case is of essentially the same form as $P(\boldsymbol{r})$.

$$<Q(\boldsymbol{r})> = \frac{1}{v}[\delta(\boldsymbol{r}-0) + P(\boldsymbol{r})] \tag{5.45}$$

The Fourier transform of the $Q(\boldsymbol{r})$ of Fig. 5.17(a) is shown in (b). $|\, S(\boldsymbol{S})\,|^2$ is concentrated predominantly about the center (Eq. 5.15), and the halos corresponding to scattering from amorphous material are observed at greater angles. Of course the convoluted form of $|\, S(\boldsymbol{S})\,|^2$ also makes its contribution to these halos.

References

1. a) D. Schechtman, I. Blech, D. Gratias, J.W. Cahn, *Phys. Rev. Lett.*, **53**, 1951 (1984).
   b) N. Wang, H. Chen, K.H. Kuo, *Phys. Rev. Lett.*, **59**, 1010 (1987).
   c) L. Bendersky, *Phys. Rev. Lett.*, **55**, 1461 (1985).
   d) T. Ishimasa, H.-U. Nissen, Y. Fukano, *Phys, Rev. Lett.*, **55**, 511 (1985); K.H. Kuo, *J. Electron Microsc. Tech.*, **7**, 277 (1987).
2. W.T. Read, Jr., *Dislocations in Crystals*, p.17, McGraw-Hill (1953).
3. R. Hosemann, *Polymer*, **3**, 349 (1962).
4. R. Hosemann, S.N. Bagchi, *Direct Analysis of Diffraction by Matter*, North-Holland Pub., Amsterdam (1962).
5. B.K. Vainshtein, *Diffraction of X-rays by Chain Molecules*, p.97, Elsevier, Amsterdam (1966).